

Bayesian and Multi-Objective Decision Support for Real-Time Cyber-Physical Incident Mitigation

Shaofei Huang, Christopher M. Poskitt, Lwin Khin Shar

Singapore Management University, Singapore

Abstract

This research proposes a real-time, adaptive decision-support framework for mitigating cyber incidents in cyber-physical systems, developed in response to an increasing reliance on these systems within critical infrastructure and evolving adversarial tactics. Existing decision-support systems often fall short in accounting for multi-agent, multi-path attacks and trade-offs between safety and operational continuity. To address this, our framework integrates hierarchical system modelling with Bayesian probabilistic reasoning, constructing Bayesian Network Graphs from system architecture and vulnerability data. Models are encoded using a Domain Specific Language to enhance computational efficiency and support dynamic updates. In our approach, we use a hybrid exposure probability estimation framework, which combines Exploit Prediction Scoring System and Common Vulnerability Scoring System scores via Bayesian confidence calibration to handle epistemic uncertainty caused by incomplete or heterogeneous vulnerability metadata. Mitigation recommendations are generated as countermeasure portfolios, refined using multi-objective optimisation to identify Pareto-optimal strategies balancing attack likelihood, impact severity, and system availability. To accommodate time- and resource-constrained incident response, frequency-based heuristics are applied to prioritise countermeasures across the optimised portfolios. The framework was evaluated through three representative cyber-physical attack scenarios, demonstrating its versatility in handling complex adversarial behaviours under real-time response constraints. The results affirm its utility in operational contexts and highlight the robustness of our proposed approach across diverse threat environments.

Keywords: cyber-physical systems, incident response, decision-support systems, multi-objective optimisation, Bayesian networks

1. Introduction

Cyber-Physical Systems (CPS) have become integral to daily life and infrastructure, enabling seamless interaction between digital and physical domains. Traditionally associated with Industrial Control Systems (ICSs), CPS are now extensively deployed in Connected and Autonomous Vehicles (CAVs), railway signalling infrastructures, and renewable energy networks. This expansion has drawn increased scrutiny toward cyber-physical security risks targeting critical infrastructure, from both attackers and defenders. In 2025, security researchers disclosed multiple vulnerabilities affecting solar photovoltaic (PV) inverters [10], highlighting how CPS components could be exploited to induce service outages, cause infrastructure damage, or in severe cases, inflict physical harm.

Given that many CPS deliver critical functions, real-time and adaptive decision support is essential for mitigating cyber incidents and minimising their impact. Here, “real-time” refers to the ability to assess and respond to threats within operational timeframes that preserve system safety and continuity, often under strict latency constraints. “Adaptive” refers to the capacity to dynamically adjust mitigation strategies based on evolving threat conditions, system states, and resource availability. However, several challenges remain. Unlike IT environments, where remediation typically involves deploying software patches or rebooting affected systems, CPS decisions must account for the interplay between cybersecurity and physical constraints [37] and take safety impacts into consideration.

In legacy systems and safety-critical applications, patching a vulnerable asset introduces significant operational risks, as poorly tested patches may lead to system failures or degraded functionality due to hardware limitations. Decision-makers must also determine the scope and extent of intervention: how much to mitigate, which assets to secure, and where to prioritise responses. These decisions are further complicated by the presence of multiple attack paths and adversary tactics, necessitating an integrated approach to countermeasure selection that balances disruption mitigation with system availability.

Recent decision-support systems (DSS) for CPS have introduced model-driven approaches leveraging simulation, system dynamics, and dependency modelling to guide risk mitigation planning [44]. While these systems support strategic assessment, they typically operate under static conditions and offer limited *adaptability* to evolving threats and system behaviours. For instance, most lack mechanisms to dynamically update model attributes, such as system properties or vulnerability exposure probabilities, during an ongoing cyber-physical incident. A typical example is the detection of a compromised communications dongle mid-

response in a power grid, where the inability to update model parameters in real time reduces operational effectiveness in time-critical scenarios.

To address these limitations, our research adopts probabilistic methodologies to enable real-time CPS decision support. We hypothesise that effective CPS incident response strategy must be guided by data-driven risk metrics and time constraints. To test this, our framework builds on: Bayesian Network (BN) models for dynamic risk management [33]; threat modelling based on Failure Modes Effects and Criticality Analysis (FMECA) [3]; a hybrid exposure probability estimation framework that synergistically integrates Common Vulnerability Scoring System (CVSS) [30] and Exploit Prediction Scoring System (EPSS) [21] scores through a novel Bayesian confidence calibration technique; the use of Domain-Specific Languages (DSLs) for semantic interoperability and computational efficiency [17]; multi-objective optimisation, coupled with frequency-based heuristic analysis, to generate risk-informed countermeasure recommendations for decision-making [45]; and finally, adaptive refinement of the model, informed by iterative assessments of observed countermeasure effectiveness.

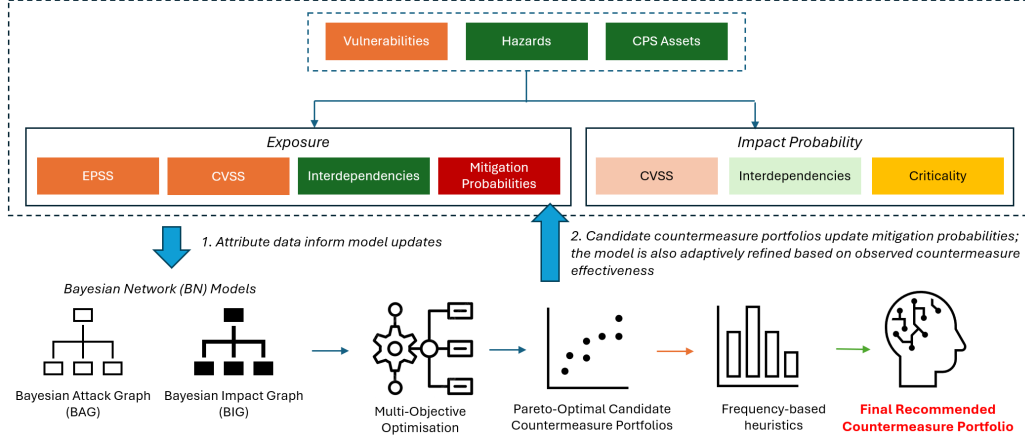


Figure 1: Architecture of our proposed framework

Our proposed framework, as depicted in Figure 1, is evaluated across three representative CPS scenarios: the 2015 Ukrainian power grid attack (BlackEnergy), a solar PV inverter system, and a railway Communication-Based Train Control (CBTC) system. Threat modelling for these scenarios was informed by the first author’s extensive cybersecurity experience in CPS, comprising 25 years of professional practice including 15 years as a Chief Information Security Officer. This depth of expertise ensured the inclusion of accurate technical insights and

domain-relevant knowledge essential for credible CPS threat representation.

Contributions. Our main contributions are:

- We propose a new way to leverage Bayesian Networks for modelling cyber attack scenarios in CPS environments. Unlike previous methods, our models are enriched with system-specific and vulnerability metadata, enabling probabilistic reasoning and risk-informed recommendations for real-time decision support. To ensure structured representation and computational efficiency, the models are encoded in a DSL format, which also facilitates dynamic updates to support adaptive decision-making in response to evolving threats.
- We use a hybrid exposure probability estimation framework that integrates the EPSS and the CVSS via a Bayesian confidence calibration technique. This framework yields robust and realistic recommendations under epistemic uncertainty stemming from incomplete or heterogeneous vulnerability metadata.
- We propose a decision-support methodology for mitigating cyber incidents in CPS, centred on countermeasure portfolios derived through multi-objective optimisation and frequency-based heuristic analysis. As a novel contribution, mitigation probabilities are treated as parameters within a structured optimisation search space, enabling the generation of Pareto-optimal portfolios that form the foundation of the decision-support mechanism. frequency-based heuristic analysis across multiple optimisation runs is further employed to prioritise mitigation strategies under time and resource constraints. The methodology is evaluated across three representative CPS attack scenarios.
- The models and source code developed in this research, along with reference data and formulae used in the framework, are publicly available via the project’s GitHub repository [18]. This supports transparency, reproducibility, and further development by both research and practitioner communities.

The remainder of this paper is structured as follows. Section 2 provides background on the key techniques adopted in this work. Section 3 outlines the proposed methodology, including its theoretical foundations and implementation

workflow, illustrated with a running example. Section 4 presents further applications of the framework to CPS attack scenarios, accompanied by an analysis of experimental results. Section 5 provides an in-depth, technical discussion of the findings and outlines directions for future research. Section 6 reviews related research and identifies limitations in existing approaches. Finally, Section 7 summarises the key contributions of the study.

2. Background

This section outlines the foundational techniques that underpin our proposed framework, including Bayesian networks, vulnerability scoring systems, and multi-objective optimisation.

Bayesian Networks. BNs are probabilistic graphical models that represent dependencies among variables using directed acyclic graphs, as illustrated in Figure 2. In cybersecurity, BNs are widely used to model attack propagation and risk inference [24], and also to support decision-making [22]. Specific to CPS, the works by Bhosale et al. [5, 6] discuss the adaptation of BN models to model probabilistic interdependencies between node types associated with CPS, namely, vulnerability nodes, which represent exploitable weaknesses in systems; asset nodes, which denote critical components within the CPS; and hazard nodes, which correspond to severe adverse outcomes including component failures.

Each of these nodes is associated with an *exposure* attribute which quantifies the likelihood that a CPS element is subject to exploitability conditions, failure dependencies, or cascading risk effects. As a critical factor in cybersecurity modelling, exposure shapes the propagation of vulnerabilities and attack vectors across interconnected CPS elements, influencing both the probability of attack success and the severity of resulting impacts. The exposure probability of each node is determined based on its attributes and its conditional dependence on parent nodes in the BN graph.

Vulnerability Scoring Systems. CVSS is a standardised framework for assessing the technical severity of software vulnerabilities, with version 3.1 defining metrics to quantify exploitability and impact characteristics [15, 30]. However, it is a deterministic scoring system that does not account for the inherent uncertainty of real-world attacks. EPSS addresses this limitation by providing a probabilistic estimate of exploitation likelihood, grounded in empirical indicators such as exploit availability, vulnerability age, and active exploitation trends in the wild [21].

EPSS complements CVSS by introducing a dynamic, data-driven layer of exposure modelling that reflects temporal threat behaviour and captures uncertainty in real-world attacks.

Multi-Objective Optimisation. CPS owners and administrators are often constrained by fixed budgets that fall short of the minimum cost required for comprehensive system hardening. The challenge lies in selecting a subset of security measures that remain within budget while minimising residual risk from unaddressed vulnerabilities. Multi-objective optimisation addresses this challenge by identifying solutions that balance competing objectives, such as cost, system availability, and risk reduction. Prior research has explored Bayesian optimisation and evolutionary strategies to derive optimal security configurations under uncertainty and resource constraints [12, 29]. In particular, the work by Zebrowski et al. [45] formulates the optimisation task as a Pareto-efficient portfolio selection problem, leveraging a Bayesian Network to represent system vulnerabilities, mitigation actions, and operational constraints that define the feasible solution space. While this approach is highly applicable to CPS environments, it can be extended to incorporate mitigation strategies that account for cascading effects, adapt to evolving attacker tactics, and support time-sensitive decision-making in dynamic threat landscapes.

3. Methodology

This section describes the methodology of our proposed framework, illustrated with a running example of a solar PV inverter attack, which is based on the security reports by Dabrowski et al. [9] and Dashevskyi et al. [10]. In particular, we refer to their identified CVEs that can be chained to form hypothetical attack paths targeting solar PV systems. While Dabrowski et al. originally proposed destabilising the power grid via coordinated load modulation from a botnet of consumer devices, our scenario explores a complementary threat vector focused on the supply side. Here, the adversary leverages mobile or web applications to obtain sensitive information, which is then used to compromise a message broker and subsequently a controller linked to both the message broker and a solar PV inverter. Once initial access is established, the attacker hijacks additional inverters and synchronises their configuration changes to create abrupt fluctuations in grid input. By overwhelming the grid’s balancing mechanisms, this coordinated attack can degrade grid stability or induce power outages, thereby achieving the attacker’s ultimate objective.

Overview. Our framework (Figure 1) begins with the construction of a BN model that defines a shared structure for attack and impact graphs, informed by CPS system attributes and the attack scenario. Randomised mitigation probability values are introduced as initial inputs into a multi-objective optimisation process, which generates candidate countermeasure portfolios aimed at maximising system availability while minimising the likelihood of attack success and severe impact occurrence. These portfolios are subsequently reintegrated into the BN as updated mitigation probabilities, and the optimisation procedure is repeated across multiple trials within a single run. The top-performing portfolios from these iterative runs are then analysed using frequency-based heuristics to identify vulnerability nodes within the attack path that consistently exhibit high mitigation effectiveness. This insight serves to guide final prioritisation decisions during incident response, particularly when confronted with stringent time and resource limitations.

The high-level steps of our proposed framework are outlined in Algorithm 1. Each step is elaborated in detail in Sections 3.1 to 3.6.

Algorithm 1 Methodology of Proposed CPS Decision Support Framework

- 1: **Build** BN model integrating CPS metadata and attack scenario context, encoded in AutomationML (§ 3.1)
 - 2: **Compute** exposure probabilities for nodes within the BN model, representing likelihoods of attack success (§ 3.2)
 - 3: **Calculate** propagated impact probabilities resulting from exploitation or failure of BN nodes (§ 3.3)
 - 4: **Calculate** posterior likelihoods of successful attack and severe impact, conditioned on observed evidence within the BN model (§ 3.4)
 - 5: **for** num_runs = 1 to max_num_runs **do**
 - 6: **for** num_trials = 1 to max_num_trials **do**
 - 7: **Run** multi-objective optimisation to generate candidate countermeasure portfolios (§ 3.5)
 - 8: **Update** BN model mitigation attributes using top-performing candidate portfolio
 - 9: **end for**
 - 10: **Identify** high-impact mitigation nodes for prioritisation under time and resource constraints, by analysing frequency-based heuristics of top-performing portfolios (§ 3.6)
 - 11: **end for**
 - 12: **Recommend** final countermeasure portfolio
-

3.1. Bayesian Network Model Construction

In the construction of a representative and abstract BN model, **nodes** denote *CPS assets*, *vulnerabilities*, and *hazards*, and **directed edges** encode causal and conditional *dependencies*. The BN model is typically constructed by domain experts or system architects with deep knowledge of the CPS architecture and operational context. This process involves identifying key system components, mapping interdependencies, and integrating vulnerability data, often sourced from CVE repositories or expert elicitation [33].

This BN model serves as a shared structural foundation for both the *Bayesian Attack Graph (BAG)* and *Bayesian Impact Graph (BIG)* models. Leveraging the defined structure, the models integrate known system information alongside hypothesised attack scenarios to instantiate asset, vulnerability, and hazard nodes within the Bayesian framework, encoded in AutomationML [13].

Running Example. Figure 2 shows a Bayesian Network representation of a solar PV inverter attack scenario. The BN model is constructed by mapping system topology and functional interdependencies referenced from the work by Dashkevskyi et al. [10]. CPS asset, vulnerability, and hazard nodes are instantiated using information from CVE repositories alongside the attack scenario [9].

3.2. Exposure Calculations

This subsection outlines our methodology used to compute probabilities of attack success, which we term as *exposures*, for vulnerability, asset, and hazard nodes within the BN representation.

Vulnerability nodes. To begin, the approach for vulnerability nodes needs to account for both publicly disclosed vulnerabilities with CVE identifiers, and proprietary or undocumented vulnerabilities lacking formal CVE enumeration. To do this, we employ an *EPSS-based formulation* for CVE-linked vulnerabilities, and a *calibrated CVSS-based fallback* for those without CVE identifiers. On the former EPSS-based formulation, the probability of exposure for a CVE-linked vulnerability is given by:

$$P(E)_{\text{vuln, EPSS}} = \text{EPSS} \quad (1)$$

where:

- $P(E)_{\text{vuln, EPSS}}$ denotes the probability that the vulnerability will be exploited.

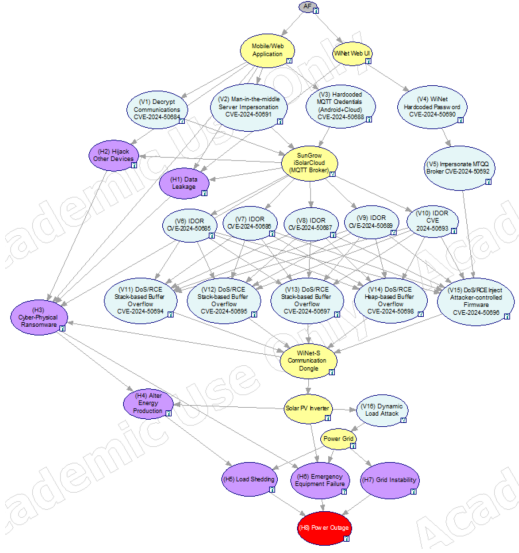


Figure 2: Bayesian Network representation of a hypothetical cyber-physical attack on solar PV inverters connected to a power grid. Nodes shaded in yellow denote CPS assets; blue nodes represent vulnerabilities; and purple nodes correspond to hazards. The grey-shaded node indicates attack feasibility, while the red-shaded node reflects the attacker’s objective, which is to cause a power outage.

- EPSS is the EPSS score retrieved from the FIRST EPSS database or API [16].

For vulnerabilities without CVE identifiers, we derive CVSS proxy estimates using the following formulation [15]:

$$P(E)_{\text{vuln, CVSS}} = AV \times AC \times PR \times UI \quad (2)$$

where each metric is assigned the corresponding numerical weight provided by FIRST [15].

Given that non-CVE vulnerabilities exhibit higher epistemic uncertainty due to limitations in CVSS scoring [40], we use a *Bayesian confidence calibration technique*, inspired by Kupperts et al. [28] to produce more realistic and robust exposure probability estimates. In our proposed formulation, both EPSS and CVSS scores are linked to a shared latent variable $P(E)_{\text{vuln}}^*$, representing the true, but unobserved, probability of exposure. These are modelled as distributions:

$$P(E)_{\text{vuln, EPSS}} \sim \mathcal{N}(P(E)_{\text{vuln}}^*, \sigma_{\text{EPSS}}^2) \quad (3)$$

$$P(E)_{\text{vuln, CVSS}} \sim \mathcal{N}(P(E)_{\text{vuln}}^*, \sigma_{\text{CVSS}}^2) \quad (4)$$

with $\sigma_{\text{CVSS}}^2 > \sigma_{\text{EPSS}}^2$, reflecting the greater epistemic uncertainty associated with CVSS scoring.

Assuming a Gaussian prior as in [25], where $P(E)_{\text{vuln}}^* \sim \mathcal{N}(\mu_0, \sigma_0^2)$, the posterior distribution over $P(E)_{\text{vuln}}^*$ can be computed analytically as:

$$\mu_{\text{post}} = \frac{\frac{\mu_0}{\sigma_0^2} + \frac{P(E)_{\text{vuln, EPSS}}}{\sigma_{\text{EPSS}}^2} + \frac{P(E)_{\text{vuln, CVSS}}}{\sigma_{\text{CVSS}}^2}}{\frac{1}{\sigma_0^2} + \frac{1}{\sigma_{\text{EPSS}}^2} + \frac{1}{\sigma_{\text{CVSS}}^2}} \quad (5)$$

$$\sigma_{\text{post}}^2 = \left(\frac{1}{\sigma_0^2} + \frac{1}{\sigma_{\text{EPSS}}^2} + \frac{1}{\sigma_{\text{CVSS}}^2} \right)^{-1} \quad (6)$$

In practice, since EPSS is unavailable for non-CVE vulnerabilities, the EPSS-related terms are omitted from the posterior update, and inference proceeds using only the prior and CVSS-derived $P(E)_{\text{vuln, CVSS}}$. The Bayesian latent variable formulation is thus represented as:

$$\mu_{\text{post}} = \frac{\frac{\mu_0}{\sigma_0^2} + \frac{P(E)_{\text{vuln, CVSS}}}{\sigma_{\text{CVSS}}^2}}{\frac{1}{\sigma_0^2} + \frac{1}{\sigma_{\text{CVSS}}^2}} \quad (7)$$

$$\sigma_{\text{post}}^2 = \left(\frac{1}{\sigma_0^2} + \frac{1}{\sigma_{\text{CVSS}}^2} \right)^{-1} \quad (8)$$

The resulting calibrated exposure probability estimate $P(E)_{\text{vuln}}^* \sim \mathcal{N}(\mu_{\text{post}}, \sigma_{\text{post}}^2)$ serves as a unified, uncertainty-aware input for downstream attack propagation and mitigation optimisation in the BN graphs.

In addition, we incorporate an attack feasibility (AF) modifier, inspired by Xie et al. [41], in the formulation to better reflect real-world conditions in subsequent probability calculations for vulnerability nodes. Specifically, the AF modifier adjusts probability estimations based on system security posture, adversary capability, and environmental constraints. Systems with up-to-date defenses and restricted access tend to reduce the likelihood of a successful attack, resulting in

lower AF values, whereas an unpatched CPS facing a skilled adversary will have a higher probability of successful attack. The final probability of successful attack of the vulnerability node is thus:

$$P(A)_{\text{vuln}} = P(E)_{\text{vuln}} \times \phi \quad (9)$$

where:

- $P(A)_{\text{vuln}}$ represents the probability that an attack of the vulnerability node is successful.
- $P(E)_{\text{vuln}}$ denotes the probability of exposure for the vulnerability.
- ϕ is the attack feasibility factor, representing context-specific factors such as system defence posture and adversary capability.

Asset nodes. For an *asset node*, the probability of exposure corresponds to the probability of asset failure and is calculated using an exponential decay function, which models failure likelihood over time:

$$P(E)_{\text{asset}} = 1 - e^{-\lambda t} \quad (10)$$

where λ represents the failure rate per unit time, determining how frequently the asset is expected to degrade, and t denotes the operational duration, reflecting the asset's time in service.

This formulation is grounded in Markov-based reliability analysis [26], wherein asset failures are modelled as a stochastic process, capturing the progressive deterioration of system components over time. By incorporating time-dependent degradation patterns, this approach provides a probabilistic estimation of failure likelihood, supporting predictive maintenance and risk-informed decision-making in CPS.

Hazard nodes. *Hazard nodes*, on the other hand, represent hazardous events, failures, or disruptions influenced by attack propagation. As such, the occurrence of a hazard is influenced by the cyber-physical dependencies within the system. If the parent node of a hazard is an asset, then the failure of that asset increases the likelihood of hazard activation. Similarly, if the parent node is another hazard, its occurrence propagates risk, potentially escalating the attack scenario.

To represent hazard occurrence probabilistically, the probability of exposure for a hazard node is defined as:

$$P(E)_{\text{haz}} = \begin{cases} 1, & \text{if parent asset fails or parent hazard occurs} \\ 0, & \text{otherwise} \end{cases} \quad (11)$$

This binary assignment ensures deterministic modeling of attack escalation and structured attack progression through hazard nodes, where asset failures or hazard dependencies directly influence security outcomes.

Running Example. In the running example, EPSS scores corresponding to the CVE identifiers of vulnerability nodes are retrieved from the FIRST EPSS database and assigned as exposure probabilities. There is however one vulnerability node, V16, that does not have a CVE identifier. In this case, we approximate the CVSS vector for V16, which denotes a dynamic load-changing attack on the power grid, based on information from the literature [9]:

CVSS:3.1/AV:N/AC:L/PR:N/UI:N/S:C/C:N/I:L/A:H

where: AV(Attack Vector):N(etwork) indicates remote exploitation over a network; AC(Attack Complexity):L(ow) reflects that no specialised conditions are required; PR(Privileges Required):N(one) and UI(User Interaction):N(one) denote that the attack requires neither privileges nor user interaction. S(Scope):C(hanged) implies that the impact extends beyond a single system, affecting the broader power grid. C(Confidentiality):N(one) indicates no confidentiality loss; I(Integrity):L(ow) reflects partial integrity compromise through unauthorised control; and A(Availabaility):H(igh) denotes a high impact on system availability, potentially leading to widespread disruption.

Using Equation 2, the fallback exposure probability estimate for V16 is calculated as:

$$P(E)_{V16, CVSS} = 0.85 \times 0.77 \times 0.85 \times 0.85 = 0.4729 \quad (12)$$

Next, we apply our Bayesian confidence calibration technique to the fallback estimate $P(E)_{V16, CVSS}$ to improve its realism and robustness. First, a standard deviation of 0.2 is assigned to reflect the low confidence level of the CVSS-proxy estimation, yielding a likelihood variance of $\sigma_{CVSS}^2 = 0.04$. For the prior distribution, a mean of $\mu_0 = 0.5$ and a variance of $\sigma_0^2 = 0.0025$ (corresponding to a standard deviation of 0.05) are assigned to reflect a neutral initial belief in the distribution. Substituting these values into Equations 7 and 8 yields the following:

$$\mu_{\text{post}} = \frac{(0.5/0.0025) + (0.4729/0.04)}{(1/0.0025) + (1/0.04)} = \frac{200 + 11.8225}{400 + 25} \approx \mathbf{0.4984} \quad (13)$$

$$\sigma_{\text{post}}^2 = \left(\frac{1}{0.0025} + \frac{1}{0.04} \right)^{-1} = (400 + 25)^{-1} = \mathbf{0.00235} \quad (14)$$

The low posterior variance of $\sigma_{\text{post}}^2 = 0.00235$ indicates that the calibrated, posterior vulnerability exposure probability estimate of $\mu_{\text{post}} \approx 0.4984$ can be used with relatively high confidence.

Additionally, an AF modifier of 1 is applied to all vulnerability node exposure probabilities using Equation 9 to reflect an idealised modelling assumption in which the adversary possesses unrestricted access and capability, and the target system exhibits minimal defensive barriers.

To calculate asset node exposure probabilities using Equation 10, the operational duration of all assets is defined from 1 January 2024 to the current date, for simplicity. Failure rates for assets, such as the WiNet-S communication dongle connected to the inverter, are estimated based on published literature [5] and technical specifications of comparable components available online. Finally, Equation 11 is used to assign exposure probabilities to the corresponding hazard nodes within the BN graph.

3.3. Impact Probability Calculations

This subsection outlines our methodology for computing the propagated impact probabilities arising from exploitation or failure of vulnerability, asset, and hazards nodes within the BN graph.

Vulnerability nodes. In the case of vulnerability nodes, we use the following formulation to compute the probability of impact [15]:

$$P(\text{Impact})_{\text{vuln}} = 1 - [(1 - C) \cdot (1 - I) \cdot (1 - A)] \quad (15)$$

where:

- $P(\text{Impact})_{\text{vuln}}$ denotes the probability of severe impact associated with the vulnerability node.
- C, I, A represent the confidentiality, integrity, and availability impact metrics, respectively. For vulnerabilities that do not have CVE identifiers, the impact metrics are estimated based on available system context, attack surface semantics, or analogous vulnerabilities with similar functionality.

Asset and Hazard Nodes. In the case of asset and hazard nodes, the probability of impact is determined by the number of child nodes each individual node directly influences, reflecting its potential to propagate disruption or failure through the system [2, 5]. This is formulated as:

$$P(\text{Impact})_{\text{asset, haz}} = \frac{\text{Number of connected child nodes}}{\text{Total number of nodes in the BN graph}} \quad (16)$$

This normalised formulation ensures that the impact probability lies within the interval [0, 1], and that asset or hazard nodes with higher structural influence, through greater downstream reach, are assigned proportionally higher impacts.

Running Example. In the running example, the impact probabilities of vulnerability nodes are calculated using Equation 15 with corresponding confidentiality, integrity, and availability impact metrics drawn from the CVSS vectors. The impact probabilities of asset and hazard nodes are calculated using Equation 16 with the corresponding values derived from the BN graph.

3.4. Posterior Probability Calculations

Once the exposures and impact probabilities for vulnerability, asset, and hazard nodes are calculated, the posterior likelihood of successful attack and the probability of severe impact to the CPS – given the evidence of a vulnerability node being exploited, for example – can be derived using conditional probability formulations and Variable Elimination (VE) techniques [18].

Running Example. For the running example, the joint conditional probabilities for exposure and impact associated with the attacker’s goal: H8_Power_Outage are shown in Table 1. These values are derived from Bayesian inference computations based on estimates, posterior parameters, and updated evidence from the risk model.

Table 1: Joint Conditional Probability Table for Exposure and Impact of H8_Power_Outage

State	$\phi_{\text{Exposure}}(\text{H8_Power_Outage})$	$\phi_{\text{Impact}}(\text{H8_Power_Outage})$
(0)	0.2555	0.9153
(1)	0.7445	0.0847

The results indicate that the posterior likelihood of a successful attack (exposure) is $P(E) = 0.2555$, while the posterior probability of severe impact on the CPS is $P(I) = 0.9153$. Multiplying these yields a composite risk score of $R = P(E) \times P(I) = 23.39\%$, highlighting the potential for high-impact outcomes even when the estimated probability of attack success is relatively moderate.

3.5. Multi-Objective Optimisation

Our framework employs multi-objective optimisation to assess and weigh trade-offs between *countermeasure portfolios*, *failure probabilities*, and *impact ratings* to inform consequence-driven and risk-informed decision support in CPS.

Countermeasure Portfolios. Countermeasure portfolios are instantiated as tuples of Probability of Mitigation attributes, embedded within each vulnerability node in the BAG and BIG models. Each portfolio is defined as an ordered tuple

$$\mathbf{M} = (P(M_1), P(M_2), \dots, P(M_n))$$

comprising the mitigation probabilities $P(M_i)$ associated with each vulnerability V_i ($i = 1, 2, \dots, n$) in the BAG model. A higher mitigation probability implies a lower likelihood of successful exploitation at the corresponding node. The ordering of nodes within these tuples reflects the relative effectiveness of mitigation strategies, thereby guiding prioritisation under resource and time constraints.

Failure probabilities. The first author's experience suggests that asset failure probabilities can be influenced by mitigation-induced risks. For instance, the application of faulty or unstable security patches to a CPS asset may introduce unintended consequences, including asset failure. This complexity is exacerbated when an asset is linked to multiple vulnerabilities, each associated with distinct mitigation-related risks. In this framework, each countermeasure is associated with a risk adjustment function that governs its net contribution to asset-level failure. Accordingly, the failure probability of a CPS asset is defined as a bounded, risk-adjusted function of the mitigations applied across its associated vulnerabilities:

$$P(F_a | \mathbf{M}) = \min \left(1.0, \kappa_a \cdot \sum_{i \in \mathcal{V}_a} P(\text{Fail}_{\text{mit}}^i) \right) \quad (17)$$

where:

- $P(F_a | \mathbf{M})$ is the probability of failure for CPS asset a given the countermeasure portfolio \mathbf{M} ;

- \mathcal{V}_a is the set of vulnerabilities associated with asset a ;
- $P(\text{Fail}_{\text{mit}}^i)$ is the probability that mitigation applied to vulnerability i causes unintended adverse consequences that contribute to asset failure;
- $\kappa_a \in (0, 1]$ is a scaling constant ensuring proportionality and bounding;
- The min function ensures the total failure probability remains within the interval $[0, 1]$.

This formulation enables our framework to support dynamic risk assessments in scenarios where mitigation strategies evolve over time or new vulnerabilities are discovered.

Impact Ratings. Another important element in the framework is the Impact Rating attribute, embedded in asset and hazard nodes. This rating captures the multifaceted consequences of successful attacks across safety, operational, financial, and informational domains. It is computed using an adaptation of the formulation proposed by Amro et al. [3]:

$$\text{Impact Rating} = \sum_{j \in \{S, F, I, O, C\}} (\text{Factor}_j \cdot \text{Criticality}_j) \quad (18)$$

where:

- S: safety impact — refers to potential harm to human life or physical injury resulting from a CPS failure or security breach.
- F: financial impact — quantifies monetary losses due to CPS equipment damage, service downtime, or disrupted business operations.
- I: informational impact — relates to the compromise, loss, or exposure of sensitive data and system configurations.
- O: operational impact — reflects the degree to which core CPS functions or processes are degraded or interrupted.
- C: staging impact — indicates the ability to enable further attacks or facilitate persistence, privilege escalation, or lateral movement.
- Factor_j : the relative weight assigned to impact type j .
- Criticality_j : the criticality level associated with impact type j .

The optimisation process begins by randomly generating countermeasure portfolios, denoted as

$$\mathbf{M}^{(j)} (j = 1, 2, \dots, n)$$

Each portfolio's mitigation values are encoded into the BN model and used to infer the posterior probabilities of both attack success and severe impact on the CPS, via Bayesian inference algorithms. These probabilistic outcomes are treated as parameters within a multi-objective search space. Pareto-optimal portfolios are then identified using the Optuna library [1], balancing the competing objectives of minimising the likelihood of attack success, and at the same time, minimising the probability of severe impact and maximising CPS availability. The resulting Pareto fronts form the foundation of our proposed decision support mechanism.

Running Example. In the running example, Equation 17 is used to calculate the risk-adjusted failure probabilities of CPS assets such as the WiNet-S communication dongle, which are connected to multiple vulnerability nodes, each associated with distinct mitigation-related risks.

Equation 18 is used to calculate impact ratings. As shown in Table 2, the impact rating of the solar PV inverter is calculated to be 0.3864. This figure arises from assigning a maximum safety factor of 1.0, based on the overarching principle that safety must never be compromised, although the associated criticality is 0, as no injuries are anticipated in the event of failure. Financial impact carries a weight of 0.25 and a criticality of 0.25, signifying localised equipment damage. The informational dimension, also weighted at 0.25, presents a higher criticality of 0.75 owing to the component's role in managing system configurations that could substantially affect overall CPS security. Operationally, the component is heavily weighted (0.75) with a matching criticality of 0.75, as it directly influences CPS operations – its failure potentially leading to cascading outages or grid instability. Finally, the staging impact holds a moderate weight of 0.5 and a criticality of 0.5, denoting the component's potential to facilitate attacker persistence or lateral movement.

Finally, a multi-optimisation study is performed to identify Pareto-optimal countermeasure portfolios. The scatter plot (Figure 3) reveals a consistent curved slope across the likelihood and impact axes, with data points forming a relatively smooth trajectory that appears to ascend with increasing impact levels. This suggests a stable correlation between these dimensions, wherein higher-impact and higher-availability scenarios tend to co-occur. The continuity of the slope

Table 2: Impact Ratings for Solar PV Inverter Components

Component	F_S	S	F_F	F	F_I	I	F_O	O	F_C	C	Impact Rating
Mobile/Web App	1	0	0.25	0	0.25	0.5	0.75	0	0.5	0.25	0.0909
WiNet Web	1	0	0.25	0	0.25	0.5	0.75	0	0.5	0.25	0.0909
MQTT Broker	1	0	0.25	0	0.25	0.5	0.75	0.5	0.5	0.5	0.2727
WiNet-S Dongle	1	0	0.25	0	0.25	0.5	0.75	0.5	0.5	0.5	0.2727
PV Inverter	1	0	0.25	0.25	0.25	0.75	0.75	0.75	0.5	0.5	0.3864
Power Grid	1	0.5	0.25	0.75	0.25	0	0.75	1	0.5	0.75	0.6591

implies underlying systemic regularities, potentially driven by latent causal BN-represented structures within the CPS environment. The scatter plot also displays a plateau between approximately 0.25 and 0.30 along the Impact axis. This observation indicates that a subset of countermeasure portfolios successfully reduce the likelihood of severe impact, yet offer limited gains in CPS availability.

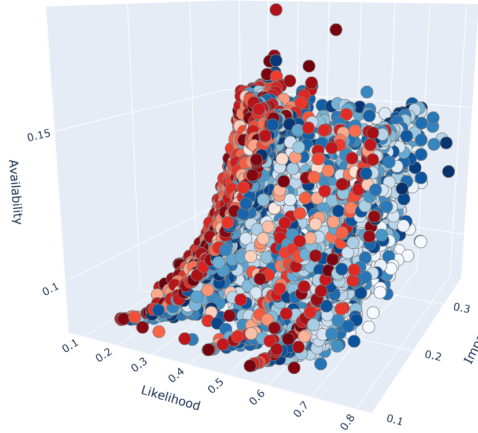


Figure 3: Pareto fronts derived over 10,000 multi-objective optimisation trials in the solar PV inverter case study

3.6. Frequency-Based Heuristic Analysis

Lastly, a frequency-based heuristic analysis of Pareto-optimal portfolios is conducted across multiple optimisation runs to rank and identify the vulnerability nodes that most consistently and effectively contributed to high-performing countermeasure configurations. These nodes are strong candidates for prioritisation in CPS mitigation strategies, particularly under time and resource constraints during incident response.

Running Example. As shown in Figure 4, vulnerabilities V1 through V4 demonstrate consistently high mitigation effectiveness across numerous portfolio instances. This finding is corroborated by the underlying Bayesian Network structure (Figure 2), which reveals that these vulnerabilities constitute critical entry points, facilitating downstream attack propagation throughout the CPS.

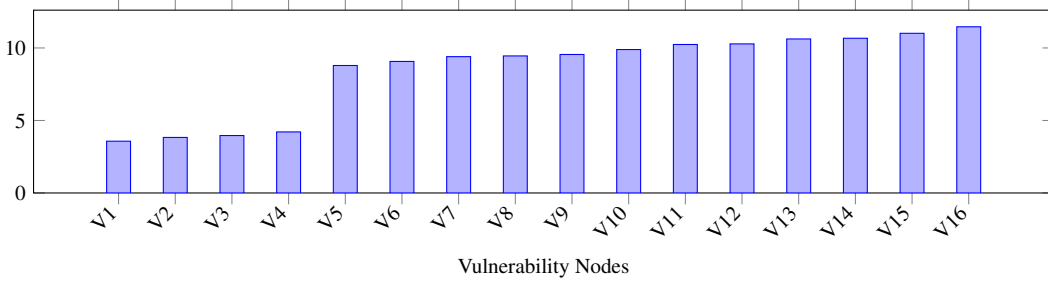


Figure 4: Average rank positions of mitigation probabilities across 100 runs of 10,000 optimisation trials in each run

In summary, the key findings of the running example of a solar PV inverter attack are:

- Optimisation results reveal systemic regularity, suggesting latent causal structures within the CPS BN structure.
- A subset of countermeasure portfolios successfully reduce the likelihood of severe impact, yet offer limited gains in CPS availability.
- Vulnerabilities V1–V4 demonstrated consistently high mitigation effectiveness, reflecting their positions as critical entry points in the CPS BN structure.

Taken together, these findings point to several practical implications for CPS practitioners. The observed systemic regularity invites further investigation into causal structures, potentially enabling more targeted interventions. Furthermore, the limited availability gains observed suggest the need for integrating complementary strategies such as anomaly detection, automated containment, or real-time system reconfiguration to strengthen operational resilience. The consistent effectiveness of vulnerabilities V1–V4 reinforces their prioritisation as part of any initial mitigation sweep, especially in scenarios involving resource-constrained decision-making.

4. Evaluation and Results

This section evaluates the practical utility and applicability of our proposed framework by applying the methodology to another two representative CPS scenarios beyond the initial case study. The corresponding results are presented and analysed to highlight key insights, limitations, and implications for real-world deployment.

4.1. Ukrainian Power Grid Attack (BlackEnergy)

Our proposed framework is applied to enable real-time, adaptive mitigation of the 2015 Ukrainian power grid attack, which notoriously leveraged the BlackEnergy malware to attack a CPS [34]. Figure 5 presents the corresponding Bayesian Network representation of the attack tree [27] created with the GeNIe Academic tool [11]. Based on this structure, the BN model is constructed using available information to define the asset, vulnerability, and hazard nodes, and encoded in AutomationML [4].

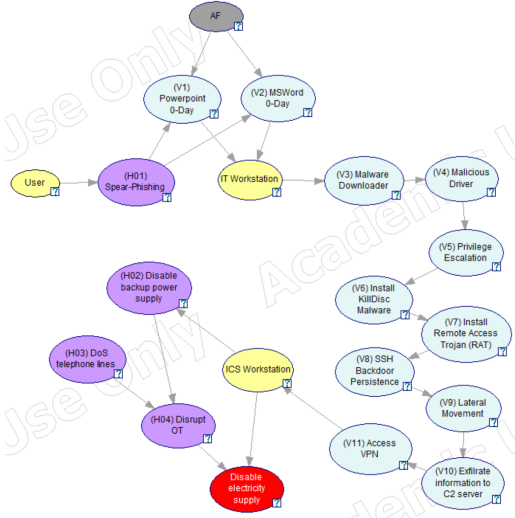


Figure 5: Bayesian Network representation of the BlackEnergy cyber attack, adapted from the attack tree model proposed by Kumar et al. [27]. Nodes shaded in yellow denote CPS assets; blue nodes represent vulnerabilities; and purple nodes correspond to hazards. The grey-shaded node indicates attack feasibility, whilst the red-shaded node reflects the attacker’s objective, which is to disrupt electricity supply.

Next, we calculate the exposure and impact probability values using the methodology outlined in Section 3. Two of the vulnerability nodes are listed in the Na-

tional Vulnerability Database (NVD) [31] and associated with CVE identifiers, whereas the remaining vulnerability nodes are not. As a fallback, the exposure probabilities of non-CVE vulnerabilities must be estimated and calibrated. Taking the example of one such vulnerability node V3, which represents a malware downloader, the CVSS-proxy vector is approximated as:

CVSS:3.1/AV:L/AC:L/PR:N/UI:N/S:U/C:H/I:H/A:H

This CVSS vector characterises a local attack scenario within the CPS: AV:L indicates the attacker requires local access to the target asset; AC:L denotes low complexity with no specialised preconditions; PR:N and UI:N indicate that exploitation requires no privileges or user interaction. S:U shows the impact is limited to the same system. The C:H, I:H, and A:H designations reflect high levels of confidentiality, integrity, and availability loss, respectively, implying complete system compromise, including access to sensitive data, arbitrary control, and potential operational failure.

Based on the CVSS vector, the exposure probability estimate is derived as:

$$P(E)_{\text{vuln, CVSS}} = 0.306 \quad (19)$$

We further calibrate this estimate using Equation 7, arriving at a corresponding likelihood variance of $\sigma_{\text{CVSS}}^2 = 0.04$ based on a standard deviation of 0.2. The low variance reflects low confidence in a heuristic-based exposure probability estimate. Additionally, the prior distribution assumes a mean of $\mu_0 = 0.5$, representing a midpoint assumption about exploitability in the absence of external evidence, and a variance of $\sigma_0^2 = 0.0025$ based on a standard deviation of 0.05, reflecting high confidence in this prior belief. Using the Bayesian latent variable formulation (cf. Equation 7), the posterior distribution is thus:

$$\mu_{\text{post}} = \frac{(0.5/0.0025) + (0.306/0.04)}{(1/0.0025) + (1/0.04)} = \frac{207.65}{425} \approx \mathbf{0.489} \quad (20)$$

$$\sigma_{\text{post}}^2 = \left(\frac{1}{0.0025} + \frac{1}{0.04} \right)^{-1} = (400 + 25)^{-1} = \mathbf{0.00235} \quad (21)$$

This yields a calibrated exposure probability estimate of approximately 0.489 with a posterior variance of 0.00235. The low posterior variance indicates that the posterior estimate can be used with relatively high confidence within the Bayesian network. Using this procedure, the calibrated exposure probability estimates for all vulnerabilities in the BlackEnergy attack model are computed.

Table 3: Joint Conditional Probability Table for Exposure and Impact of H5_Disable_Electrical_Supply

State	$\phi_{\text{Exposure}}(\text{Goal})$	$\phi_{\text{Impact}}(\text{Goal})$
(0)	0.8750	0.2393
(1)	0.1250	0.7607

Table 3 presents the conditional probabilities for exposure and impact associated with the attacker’s goal: H5_Disable_Electrical_Supply, derived using Bayesian inference via a Variable Elimination algorithm. The results show a posterior likelihood of successful attack of $P(E) = 0.875$, and a corresponding posterior probability of severe impact on the CPS of $P(I) = 0.2393$. The composite risk score is computed as $R = P(E) \times P(I) = 20.94\%$ in the BlackEnergy attack.

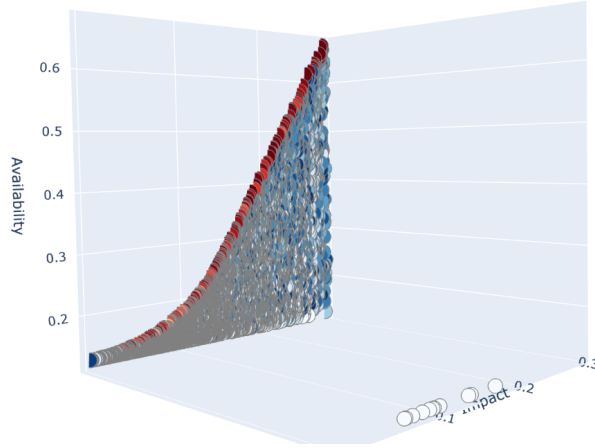


Figure 6: Pareto fronts derived over 10,000 optimisation trials in the BlackEnergy case study. Countermeasure portfolios were optimised to minimise both the likelihood of a successful attack and the probability of severe impact in CPS, while maximising CPS availability.

Next, we performed optimisation studies to search for Pareto-optimal countermeasure portfolios to support decision-making in mitigating the BlackEnergy attack. Figure 6 reveals an increasingly linear relationship between impact probability and CPS availability at higher impact probability levels. Additionally, the Pareto fronts appear clustered near a similar value along the attack likelihood axis, suggesting limited variation in attack likelihood across trials.

Table 4: Top-performing countermeasure portfolio from the BlackEnergy case study. The countermeasure portfolio was optimised to minimise the likelihood of attack success and severe impact, while maximising CPS availability.

Metric	Value
Trial ID	9683
Countermeasure portfolio	V1:0.9901, V2:0.9855, V3:0.9777, V4:0.9821, V5:0.9954, V6:0.9892, V7:0.9824, V8:0.9903, V9:0.9713, V10:0.9722, V11:0.9772
Likelihood of successful attack	0.1486
Probability of severe impact	0.2899
Availability	0.6766

Inspection of the top-performing countermeasure portfolio (Table 4) reveal near-maximal intervention against all vulnerabilities, with all mitigation parameters close to 1.0. Despite this, the probability of severe impact remained moderate. This suggests that in the case of the BlackEnergy attack, aggressive mitigation improves system availability, but does not fully suppress the residual risk of severe impact on the CPS.

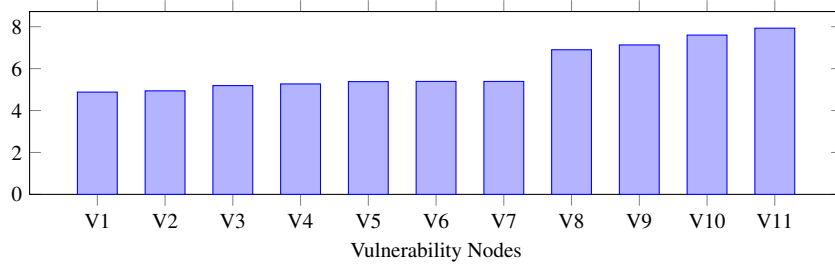


Figure 7: Average rank positions of mitigation probabilities across 100 runs of 10,000 optimisation trials in each run. Nodes are ranked based on the relative magnitude of their mitigation probabilities in the optimal portfolios, with rank 1 indicating the highest mitigative effectiveness.

Lastly, we conducted a frequency-based heuristic analysis of Pareto-optimal portfolios across multiple optimisation runs to identify and recommend countermeasures that best mitigate the BlackEnergy attack. As shown in Figure 7, vulnerabilities V1 through V7 exhibit relatively similar bar heights, indicating that mitigation must adopt a distributed strategy across multiple vulnerability nodes concurrently.

Such a strategy inherently demands greater resource investment and operational effort. In contrast, applying mitigations only to a limited subset of the countermeasure portfolio, such as V1 and V2, delivers only partial effectiveness.

In this scenario, if just two of the seven top-ranked mitigations are implemented, the estimated mitigation effectiveness is approximately $2/7 \times 100 = 28.57\%$ of that should the full portfolio be implemented. This highlights the limitation of narrow mitigation strategies, which risk leaving critical attack paths unaddressed.

In summary, the key findings from the framework’s application to the Ukrainian power grid attack are:

- Increasingly linear relationship between impact probability and CPS availability at higher impact probability levels.
- Pareto fronts appear clustered near a similar value along the attack likelihood axis, suggesting limited variation in attack likelihood across optimisation trials.
- Aggressive mitigation improves availability, but does not fully suppress the residual risk of severe impact on the CPS.
- Mitigation must adopt a distributed strategy across multiple vulnerability nodes concurrently.

These insights equip CPS practitioners with the rationale to adopt a multi-pronged mitigation strategy tailored to the dynamics of BlackEnergy-like threats. Firstly, CPS practitioners should invest in early-stage interventions to reduce exposure before the system enters high-risk zones. Secondly, the clustering of Pareto fronts around similar attack likelihood values calls for prioritising interventions based on impact severity and system availability, rather than likelihood alone. Even when near-total mitigation coverage is pursued aggressively, residual risks may persist. This warrants the need to complement countermeasure portfolios with real-time anomaly detection, automated containment mechanisms, or fail-safe protocols to arrest cascading failures. Finally, CPS practitioners should adopt mitigation strategies designed to target multiple vulnerabilities in parallel to enhance CPS resilience.

4.2. Railway CBTC System Attack

Next, we shift our focus to a cyber-physical attack scenario involving a railway CBTC system. To construct a plausible threat model, we draw upon the first author’s years of expertise and domain-specific knowledge of railway CBTC systems, complemented by insights from literature that discuss CBTC architecture, vulnerabilities, and risk assessment methods. Synthesising these insights,

we formulate a hypothetical cyber-physical attack path that targets CBTC assets through a chain of associated cyber-physical vulnerabilities. These relationships are instantiated within a Bayesian Network model, as illustrated in Figure 8.

Figure 8: Bayesian Network representation of a hypothetical cyber-physical attack on a railway CBTC system. Nodes shaded in yellow denote CPS assets; blue nodes represent vulnerabilities; and purple nodes correspond to hazards. The grey-shaded node indicates attack feasibility, while the red-shaded node reflects the attacker’s objective, which is to disrupt train operation.

Table 5 presents a side-by-side comparison of the conditional probability distributions for exposure and impact associated with the attacker’s goal: `H3_Disrupt_Train_Operation`, derived from both CVSS-based and EPSS-based prior distributions. Notably, the EPSS-based result closely mirrors the CVSS-based result, suggesting that both scoring systems yield similar risk estimates for this attack scenario.

Table 5: Comparison of Joint Conditional Probabilities for Exposure and Impact of H3_Disrupt_Train_Operation Based on CVSS and EPSS Prior Distributions

State	CVSS-Based		EPSS-Based	
	ϕ_{Exposure}	ϕ_{Impact}	ϕ_{Exposure}	ϕ_{Impact}
(0)	0.1256	1.0000	0.1254	1.0000
(1)	0.8744	0.0000	0.8746	0.0000

The CVSS-based result indicates a posterior probability of attack success of $P(E) = 0.1256$ and a conditional probability of severe impact of $P(I) = 1.0000$, yielding a composite risk score of $R = P(E) \times P(I) = 12.56\%$. While this score is relatively modest, the analysis reveals full certainty of a critical system impact if the attack path is realised. This suggests a need for further consideration of preventive strategies tailored to this attack scenario.

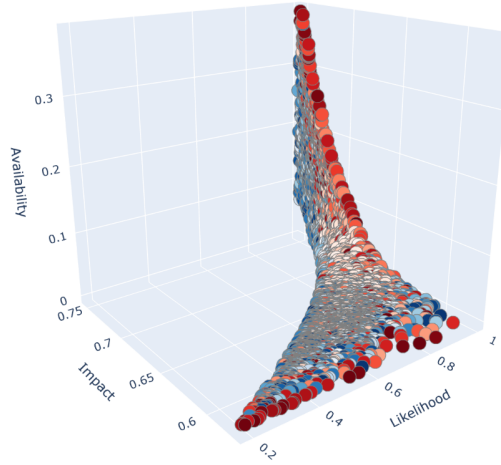


Figure 9: Pareto fronts derived over 10,000 multi-objective optimisation trials in the railway CBTC case study

Next, we conducted optimisation experiments, separately using calibrated CVSS-based priors and EPSS-based priors, to evaluate differences in outcomes. In both cases, the Pareto fronts (Figure 9) reveal a consistent linear relationship between the probability of severe impact and CPS availability at elevated impact levels. Dense solution clusters are also observed near $Likelihood = 1$ and $Impact = 1$, indicating strong model confidence that attacks are likely to succeed under most mitigation configurations. This suggests that the optimisation process prioritises

improvements in CPS availability, rather than prevent compromise altogether.

Table 6: Comparison of top-performing countermeasure portfolios from the railway CBTC case study using calibrated CVSS-based and EPSS-based priors

Metric	CVSS-based (Trial 8361)	EPSS-based (Trial 9234)
Countermeasure portfolio	V1:0.9986, V2:0.9883, V3:0.9788, V4:0.9994, V5:0.9929, V6:0.9961, V7:0.9579, V8:0.9914	V1:0.9759, V2:0.9778, V3:0.9792, V4:0.9835, V5:0.9942, V6:0.9873, V7:0.9862, V8:0.9532
Probability of severe impact	0.7581	0.7559
Availability	0.4694	0.4462
Total execution time	0h 4m 31s	0h 4m 23s

The top-performing countermeasure portfolios are presented in Table 6. The solutions reflect a broad system-wide defence strategy in the scenario of a railway CBTC attack, with near-maximal mitigation across all variables. Although the calibrated CVSS-based solution achieves marginally higher availability (0.4694 vs. 0.4462), the EPSS-based trial exhibits a slightly lower probability of severe impact (0.7559 vs. 0.7581).

Lastly, we analysed Pareto-optimal portfolios obtained from repeated optimisation runs using both calibrated CVSS-based and EPSS-based priors, applying a frequency-based ranking to identify which vulnerability nodes were most consistently selected for Pareto-optimal countermeasure portfolios. There were visible differences between results derived from calibrated CVSS-based and EPSS-based priors respectively. As illustrated in Figure 10, the calibrated CVSS-based distribution exhibits a largely uniform pattern, with V1 exhibiting the strongest mitigation effect. In contrast, the EPSS-based distribution is more varied, with V3, V6, and V7 exhibiting higher mitigation effects relative to other nodes.

In summary, the key findings from the framework’s application to the railway CBTC system attack are:

- No marked differences between optimisation results based on EPSS and CVSS priors, respectively.
- Optimisation results favour system availability over attack prevention.
- Countermeasure portfolios show near-maximal mitigation across all vulnerabilities, reflecting a system-wide defence approach.

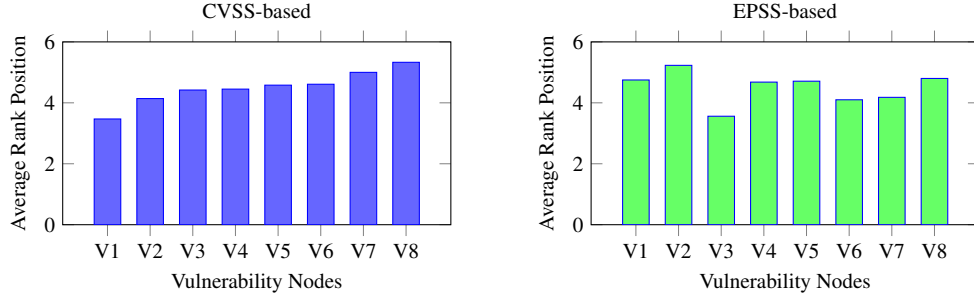


Figure 10: Side-by-side comparison of average mitigation rank positions across 100 optimisation runs (10,000 trials each) using calibrated CVSS-based and EPSS-based priors. Lower values indicate higher mitigative effectiveness.

- Frequency analysis shows uniform emphasis in countermeasure portfolios derived from calibrated CVSS-based priors, while portfolios derived from EPSS-based priors indicate more targeted mitigation strategies.

These observations provide useful guidance for CPS practitioners. Importantly, the results suggest flexibility in using EPSS and CVSS in scenarios where none of the vulnerabilities are linked to known CVEs. Frequency analysis can further support comparative evaluation of CVSS- and EPSS-based results, enabling selection of more targeted mitigation strategies tailored to meet tight resource and real-time constraints in CPS incidents.

5. Discussion and future work

Framework applicability to real-world attacks. All three case studies, including the solar PV inverter running example in Section 3, demonstrate the applicability and utility of our proposed framework in supporting real-time, adaptive decision-making needs for real-world attacks. As new information becomes available, elements such as CPS assets, probabilistic estimates of attack likelihood, impact severity, system availability, and candidate countermeasure profiles, comprising mitigation probabilities, are continuously updated via a feedback loop driven by real-time monitoring and computationally efficient multi-objective optimisation. Future work could further investigate how CVSS-based priors, both calibrated and non-calibrated, and probabilistic EPSS-based priors affect multi-objective optimisation outcomes in CPS contexts.

Repeatability of optimisation outcomes. An important consideration arising from our research concerns the repeatability of outcomes, such as countermeasure portfolios, produced by multi-objective optimisation trials in response to identical model configurations and threat information. This directly relates to the stability and variance of Pareto fronts across repeated optimisation runs. To evaluate this, we pose the question: *What configuration of trial count is sufficient to ensure that the resulting Pareto front remains relatively consistent across independent multi-objective optimisation runs?*

To address this research question, we evaluated the nearness and clustering behaviour of Pareto fronts generated from 100, 1000, 5000, and 10,000 trials, each repeated over 100 optimisation runs. Comparison of the Pareto fronts across experimental configurations reveals that lower trial counts (e.g. 100) result in considerable dispersion and variability across runs, whereas higher trial counts (e.g. 5000 and 10,000) yield denser, more structurally consistent front distributions across objective space.

To derive a quantitative measure and comparison of cluster density, Kernel Density Estimation (KDE) [7] was employed, following a validation of unimodality of the distributions of attack likelihood, impact probability, and availability. The KDE-derived density metrics are summarised in Table 7. Taken together, these findings support the conclusion that a configuration of at least 5,000 trials is sufficient to generate consistent and structurally reliable Pareto fronts across independent multi-objective optimisation runs. However, for applications demanding finer resolution or more robust density differentiation, such as real-time countermeasure ranking or adaptive planning, a 10,000-trial configuration may offer marginally improved fidelity, albeit at the expense of execution time.

Table 7: Comparison of KDE-derived density metrics for Pareto-optimal solutions across trial configurations (100 runs each)

Metric	100 trials	1,000 trials	5,000 trials	10,000 trials
Average KDE	601.17	543.70	359.65	395.99
Minimum density	136.64	51.13	31.01	45.91
Maximum density	1130.66	1041.85	698.14	887.52
Density variance	62,435.93	84,427.79	36,824.83	56,210.58
Density entropy	4.51	4.44	4.43	4.40

Concurrency and computational efficiency. The optimisation experiments conducted in this research underscore the critical role of concurrency in enhancing

computational efficiency and responsiveness for multi-objective decision-making in CPS. Using the Python `concurrent.futures` module, we achieved substantial reductions in cumulative optimisation time (Table 8).

Table 8: Comparison of execution times for 3 runs of 10,000 trials each

Configuration	Optuna	Optuna + <code>concurrent.futures</code>
Total execution time	15 mins 3 secs	5 mins 10 secs

Future work. To further strengthen real-time decision-making capabilities in CPS, future work should explore several complementary directions that address the key challenges identified in our research.

First, our research highlighted the promise of frequency-based heuristics as a supplementary analytical layer beyond individual optimisation outcomes. However, their empirical nature prompts a critical question: *To what extent can such heuristically derived recommendations be relied upon in real-time, safety-critical CPS environments?* Addressing this question presents a valuable avenue for future work, particularly through comparative evaluation with empirical data.

Secondly, the stability of Pareto fronts across repeated optimisation trials remains central to ensuring decision robustness. Low trial counts were shown to produce high variance in outcomes, which may undermine the trustworthiness of mitigation recommendations. Future investigations should therefore develop convergence diagnostics to establish sufficiency thresholds for trial configurations, and to measure the robustness of optimisation solutions.

Thirdly, the incorporation of hybrid EPSS–CVSS exposure probability assessments, as proposed in our research, presents a promising direction for improving vulnerability assessment. Such hybrid models are particularly well suited to guiding mitigation strategies that must adapt in real time to both known vulnerabilities and evolving threat intelligence.

Finally, architectural improvements and mechanisms could be explored to dynamically rebalance the factors employed in impact calculations (as outlined in Section 3.3), thereby enabling the generation of countermeasure portfolios that reflect evolving runtime priorities. This may include structural enhancements such as the incorporation of noisy-OR gates to improve agility in assimilating new evidence, and to better support adaptive decision-making.

Collectively, these directions aim to further improve a real-time, adaptive decision support framework for mitigating cyber incidents in CPS.

6. Related work

BNs for Decision-Making. BNs have proven effective in synthesising heterogeneous data for cybersecurity modelling, particularly where historical attack data is scarce [8, 20]. Prior studies [41, 33, 39, 23] demonstrate their value for dynamic decision-making. Bhosale et al. [5, 6] further integrate hazard, vulnerability, and asset connectivity into Bayesian Belief Networks (BBNs), supported by AutomationML for real-time data exchange.

Nonetheless, existing frameworks do not account for the unintended consequences of CPS mitigations, such as asset degradation or failure from software patching, and do not account for legacy system constraints and resource limitations. Their reliance on CVSS v3.1 also limits adaptability to evolving threats, where EPSS [21] offers complementary probabilistic insight. Crucially, these models lack feedback mechanisms to iteratively refine risk postures in response to new threats.

Our research addresses these gaps by proposing a consequence-aware, iterative framework that couples hybrid CVSS-EPSS exposure probability estimation with adaptive decision-support for CPS security.

Consequence-driven Security Assessment. In addition to modelling attack propagation, effective CPS decision-making must account for the consequences of cyber-physical attacks. Kim et al. [24] incorporate a consequence layer within BN models to quantify impact propagation in exploited ICSs, detailing functional interdependencies and infrastructure-wide effects. ACTISM [19] similarly adopts a consequence-driven approach for dynamic, iterative security modelling in automotive systems. In parallel, Amro et al. [3] propose a consequence-driven framework rooted in FMECA, well-aligned with CPS environments.

Although these approaches support iterative risk assessment, their transformation into adaptive decision-support tools hinges on modelling realistic, multi-stage cyber-physical attacks. To meet this challenge, our research integrates system-level and functional dependencies into BN structures informed by real-world scenarios, and explicitly models uncertainty within exposure computations. Together, these enhancements extend consequence-aware modelling toward responsive CPS decision-making under evolving threat landscapes.

DSS for CPS. Research has explored diverse methodologies for real-time CPS decision-making under uncertainty. Zaman et al. [44] propose a Markov Decision Process (MDP) framework for optimising responses to hazards such as fire outbreaks and power outages using CPS data. Javornik et al. [22] introduce a mission-

centric decision support system to guide cybersecurity experts in selecting resilient IT configurations in stakeholder-driven contexts. While both frameworks offer structured resilience assessments, they do not account for CPS-specific constraints, adversary tactics, and cascading cyber-physical risks.

To address these limitations, our research employs BN structures with nodes representing CPS assets, vulnerabilities, and hazards, along with their interdependencies. This approach facilitates dynamic modelling of risk propagation and supports adaptive decision-making that reflects evolving threat scenarios and system-level complexity.

Multi-Objective Optimisation. Decision-making in CPS cyber incident response must balance cybersecurity, safety, and operational continuity. Li et al. [29] propose a multi-objective optimisation framework for intrusion response in ICSs, prioritising Pareto-optimal security strategies using a distance-based metric. However, it does not account for unknown vulnerabilities or emerging attack vectors, limiting responsiveness in dynamic environments. Zebrowski et al. [45] present a similar optimisation-based approach using Bayesian Networks to assess cascading cyberattack impacts and minimise catastrophic consequences. Yet, their framework assumes static cybersecurity configurations and lacks adaptability to evolving threats.

To address these limitations, our research uses a Bayesian confidence calibration technique to model uncertainty from unknown or emerging attack vectors. It also implements an iterative countermeasure portfolio refinement cycle, guided by feedback from previously evaluated mitigation strategies. These innovations support the development of adaptive, context-aware CPS security strategies tailored for real-time decision-making under uncertainty.

Railway CBTC Systems. Several studies have examined railway signalling security, with varying emphasis on CBTC systems. Xu et al. [42] present a simulation platform architecture grounded in real-world CBTC characteristics. In contrast, Schlehuber et al. [35] focus on interlocking systems without addressing CBTC explicitly, and Unger et al. [38] survey railway attack scenarios and countermeasure maturity, yet do not concentrate on CBTC systems. Conversely, Yu et al. [43] offer a comprehensive review of CBTC architecture, limitations, cybersecurity threats, and protection strategies.

Regarding systemic vulnerabilities, Farooq et al. [14] analyse over-the-air communications in CBTC, identifying interference susceptibility, particularly in Wi-Fi technologies. Oliveira et al. [32] echo this concern, using Failure Mode and

Effects Analysis (FMEA) to uncover risks such as message spoofing and MitM attacks that compromise communication integrity. Similarly, Soderi et al. [36] outline wireless attack scenarios with demonstrated impacts on railway safety. These findings directly inform the attack modelling applied in the CBTC case study presented in this paper.

7. Conclusion

We presented a real-time, adaptive decision support framework for mitigating cyber incidents in CPS environments. Its development is timely, given the growing reliance on CPS within critical infrastructure, and the rapidly evolving cyber threat landscape.

A key contribution of this work is the use of BN models to represent attack scenarios, enriched with CPS system and vulnerability metadata to facilitate probabilistic reasoning and risk-informed recommendations for real-time incident response. The models are encoded in a DSL format to enhance computational efficiency under operational constraints, and to support dynamic updates for adaptive decision support.

We also introduced a novel decision-support methodology centred on counter-measure portfolios derived through multi-objective optimisation and frequency-based heuristic analysis. Mitigation probabilities are treated as parameters within a structured optimisation search space, allowing the generation of Pareto-optimal portfolios that balance system availability, attack success likelihood, and impact severity. frequency-based heuristic analysis across multiple optimisation runs is further employed to identify consistently effective mitigation nodes, thereby guiding prioritisation decisions under time and resource constraints.

Additionally, we used a hybrid exposure probability estimation technique that integrates EPSS and CVSS scores via Bayesian confidence calibration. This approach yields robust and realistic exposure recommendations under epistemic uncertainty arising from incomplete or heterogeneous vulnerability data.

The framework was evaluated across three representative CPS attack scenarios, encompassing both multi-path and multi-agent threats. Collectively, these evaluations demonstrate the framework’s utility in supporting real-time, adaptive decision-making for cyber incident mitigation in CPS environments.

CRediT authorship contribution statement

Shaofei Huang: Conceptualisation, Methodology, Software, Validation, Formal analysis, Investigation, Writing – Original Draft, Writing – Review & Editing,

Visualisation, Project administration. **Christopher M. Poskitt:** Conceptualisation, Methodology, Writing – Review & Editing, Supervision. **Lwin Khin Shar:** Conceptualisation, Methodology, Writing – Review & Editing, Supervision.

Declaration of Competing Interest

The authors declare that there are no conflicts of interest that could have influenced the conduct or outcomes of this research. Furthermore, this research did not receive any specific grant from funding agencies in the public, commercial, or not-for-profit sectors.

Data Availability

The models and source code developed as part of this research are publicly available via the project’s GitHub repository ([18]).

References

- [1] Akiba, T., Sano, S., Yanase, T., Ohta, T., Koyama, M., 2019. Optuna: A next-generation hyperparameter optimization framework, in: Proceedings of the 25th ACM SIGKDD international conference on knowledge discovery & data mining, pp. 2623–2631. doi:10.1145/3292500.333070.
- [2] Akoglu, L., Tong, H., Koutra, D., 2015. Graph based anomaly detection and description: a survey. *Data mining and knowledge discovery* 29, 626–688. doi:10.1007/s10618-014-0365-y.
- [3] Amro, A., Gkioulos, V., Katsikas, S., 2023. Assessing cyber risk in cyber-physical systems using the att&ck framework. *ACM Transactions on Privacy and Security* 26, 1–33. doi:10.1145/3571733.
- [4] AutomationML Association, 2025. AutomationML Editor. <https://github.com/AutomationML/AutomationMLEditor>. Accessed: 2025-08-31.
- [5] Bhosale, P., Kastner, W., Sauter, T., 2023. Integrated safety-security risk assessment for production systems: A use case using bayesian belief networks, in: 2023 IEEE 21st International Conference on Industrial Informatics (INDIN), IEEE. pp. 1–6. doi:10.1109/INDIN51400.2023.10217926.

- [6] Bhosale, P., Kastner, W., Sauter, T., 2024. AutomationML meets Bayesian Networks: A Comprehensive Safety-Security Risk Assessment in Industrial Control Systems. *IEEE Open Journal of the Industrial Electronics Society* doi:10.1109/OJIES.2024.3439388.
- [7] Chen, Y.C., 2017. A tutorial on kernel density estimation and recent advances. *Biostatistics & Epidemiology* 1, 161–187. doi:10.1080/24709360.2017.1396742.
- [8] Chockalingam, S., Pieters, W., Teixeira, A., van Gelder, P., 2017. Bayesian network models in cyber security: a systematic review, in: *Secure IT Systems: 22nd Nordic Conference, NordSec 2017, Tartu, Estonia, November 8–10, 2017, Proceedings 22*, Springer. pp. 105–122. doi:10.1007/978-3-319-70290-2_7.
- [9] Dabrowski, A., Ullrich, J., Weippl, E.R., 2017. Grid shock: Coordinated load-changing attacks on power grids: The non-smart power grid is vulnerable to cyber attacks as well, in: *Proceedings of the 33rd Annual Computer Security Applications Conference*, pp. 303–314. doi:10.1145/3134600.313463.
- [10] Dashevskiy, S., La Spina, F., Dos Santos, D., 2025. SUN:DOWN Destabilizing the grid via orchestrated exploitation of solar power systems. <https://www.forescout.com/resources/sun-down-research-report/>. Accessed: 2025-08-31.
- [11] Decision Systems Laboratory, 2023. GeNie Modeler. <https://www.bayesfusion.com/genie/>. BayesFusion, LLC. Accessed: 2025-08-31.
- [12] Dewri, R., Poolsappasit, N., Ray, I., Whitley, D., 2007. Optimal security hardening using multi-objective optimization on attack tree models of networks, in: *Proceedings of the 14th ACM conference on Computer and communications security*, pp. 204–213. doi:10.1145/1315245.1315272.
- [13] Drath, R., Luder, A., Peschke, J., Hundt, L., 2008. Automationml-the glue for seamless automation engineering, in: *2008 IEEE International Conference on Emerging Technologies and Factory Automation*, IEEE. pp. 616–623. doi:10.1109/ETFA.2008.4638461.

- [14] Farooq, J., Soler, J., 2017. Radio communication for communications-based train control (CBTC): A tutorial and survey. *IEEE Communications Surveys & Tutorials* 19, 1377–1402. doi:10.1109/COMST.2017.2661384.
- [15] FIRST, 2015. Common Vulnerability Scoring System v3.1: Specification Document. <https://www.first.org/cvss/v3-1/specification-document>. Accessed: 2025-08-31.
- [16] FIRST, 2025. Open Source EPSS Tools. https://www.first.org/epss/epss_tools. Accessed: 2025-08-31.
- [17] Fowler, M., 2010. Domain-specific languages. Pearson Education.
- [18] Huang, S., 2025. Project Repository: Bayesian and Multi-Objective Decision Support for Real-Time Cyber-Physical Incident Mitigation. https://github.com/shaofeihuang/CPS_BayesianMODS. Accessed: 2025-08-31.
- [19] Huang, S., Poskitt, C.M., Shar, L.K., 2024a. ACTISM: Threat-informed Dynamic Security Modelling for Automotive Systems. *arXiv preprint arXiv:2412.00416* doi:10.48550/arXiv.2412.00416.
- [20] Huang, S., Poskitt, C.M., Shar, L.K., 2024b. Security Modelling for Cyber-Physical Systems: A Systematic Literature Review. *arXiv preprint arXiv:2404.07527* doi:10.48550/arXiv.2404.07527.
- [21] Jacobs, J., Romanosky, S., Edwards, B., Adjerid, I., Roytman, M., 2021. Exploit Prediction Scoring System (EPSS). *Digital Threats: Research and Practice* 2, 1–17. doi:10.1145/3436242.
- [22] Javorník, M., Husák, M., 2022. Mission-centric decision support in cybersecurity via Bayesian Privilege Attack Graph. *Engineering Reports* 4, e12538. doi:10.1002/eng2.12538.
- [23] Khosravi-Farmad, M., Ghaemi-Bafghi, A., 2020. Bayesian decision network-based security risk management framework. *Journal of Network and Systems Management* 28, 1794–1819. doi:10.1007/s10922-020-09558-5.

- [24] Kim, A., Oh, J., Kwon, K., Lee, K., 2022. Consider the consequences: A risk assessment approach for industrial control systems. *Security and Communication Networks* 2022, 3455647. doi:10.1155/2022/3455647.
- [25] Knapik, B.T., van der Vaart, A.W., van Zanten, J.H., 2011. Bayesian inverse problems with Gaussian priors. *The Annals of Statistics* 39, 2626 – 2657. doi:10.1214/11-AOS920.
- [26] Kumar, A., Saini, M., Saini, D.K., Badiwal, N., 2021. Cyber physical systems-reliability modelling: critical perspective and its impact. *International Journal of System Assurance Engineering and Management* 12, 1334–1347. doi:10.1007/s13198-021-01305-6.
- [27] Kumar, R., Kela, R., Singh, S., Trujillo-Rasua, R., 2022. APT attacks on industrial control systems: A tale of three incidents. *International Journal of Critical Infrastructure Protection* 37, 100521. doi:10.1016/j.ijcip.2022.100521.
- [28] Küppers, F., Kronenberger, J., Schneider, J., Haselhoff, A., 2021. Bayesian confidence calibration for epistemic uncertainty modelling, in: 2021 IEEE Intelligent Vehicles Symposium (IV), IEEE. pp. 466–472. doi:10.1109/IV48863.2021.9575841.
- [29] Li, X., Zhou, C., Tian, Y.C., Qin, Y., 2018. A dynamic decision-making approach for intrusion response in industrial control systems. *IEEE Transactions on Industrial Informatics* 15, 2544–2554. doi:10.1109/TII.2018.2866445.
- [30] Mell, P., Scarfone, K., Romanosky, S., 2007. Common vulnerability scoring system. *IEEE Security & Privacy* 4, 85–89. doi:10.1109/MSP.2006.145.
- [31] NIST, 2025. National Vulnerability Database. <https://nvd.nist.gov/>. Accessed: 2025-08-31.
- [32] Oliveira, J., Carvalho, G., Cabral, B., Bernardino, J., 2020. Failure mode and effect analysis for cyber-physical systems. *Future Internet* 12, 205. doi:10.3390/fi12110205.
- [33] Poolsappasit, N., Dewri, R., Ray, I., 2011. Dynamic security risk management using Bayesian Attack Graphs. *IEEE Transactions on Dependable and Secure Computing* 9, 61–74. doi:10.1109/TDSC.2011.34.

- [34] SANS, 2016. Analysis of the cyber attack on the Ukrainian power grid. Electricity Information Sharing and Analysis Center (E-ISAC) 388, 3.
- [35] Schlehuber, C., Heinrich, M., Vateva-Gurova, T., Katzenbeisser, S., Suri, N., 2017. A security architecture for railway signalling, in: Computer Safety, Reliability, and Security: 36th International Conference, SAFECOMP 2017, Trento, Italy, September 13-15, 2017, Proceedings 36, Springer. pp. 320–328. doi:10.1007/978-3-319-66266-4_21.
- [36] Soderi, S., Masti, D., Hämäläinen, M., Iinatti, J., 2023. Cybersecurity considerations for Communication Based Train Control. IEEE Access 11, 92312–92321. doi:10.1109/ACCESS.2023.3309005.
- [37] Taylor, J.M., Sharif, H.R., 2017. Security challenges and methods for protecting critical infrastructure cyber-physical systems, in: 2017 International Conference on Selected Topics in Mobile and Wireless Networking (MoWNeT), pp. 1–6. doi:10.1109/MoWNeT.2017.8045959.
- [38] Unger, S., Heinrich, M., Scheuermann, D., Katzenbeisser, S., Schubert, M., Hagemann, L., Iffländer, L., 2023. Securing the future railway system: Technology forecast, security measures, and research demands. Vehicles 5, 1254–1274. doi:10.3390/vehicles5040069.
- [39] Wang, L., Jajodia, S., Singhal, A., Frigault, M., Wang, L., Jajodia, S., Singhal, A., 2017. Measuring the overall network security by combining CVSS scores based on attack graphs and Bayesian networks. Network Security Metrics , 1–23doi:10.1007/978-3-319-66505-4_1.
- [40] Wunder, J., Kurtz, A., Eichenmüller, C., Gassmann, F., Benenson, Z., 2024. Shedding light on cvss scoring inconsistencies: A user-centric study on evaluating widespread security vulnerabilities, in: 2024 IEEE Symposium on Security and Privacy (SP), IEEE. pp. 1102–1121. doi:10.1109/SP54263.2024.00058.
- [41] Xie, P., Li, J.H., Ou, X., Liu, P., Levy, R., 2010. Using bayesian networks for cyber security analysis, in: 2010 IEEE/IFIP international conference on dependable systems & networks (DSN), IEEE. pp. 211–220. doi:10.1109/DSN.2010.5544924.

- [42] Xu, J., Chen, L., Gao, W., Zhao, M., et al., 2015. Cbtc simulation platform design and study. *Journal of Computer and Communications* 3, 61. doi:10.4236/jcc.2015.39007.
- [43] Yu, Z., Wang, H., Chen, F., 2023. Security of railway control systems: A survey, research issues and challenges. *High-speed Railway* 1, 6–17. doi:10.1016/j.hspr.2022.12.001.
- [44] Zaman, M., Eini, R., Zohrabi, N., Abdelwahed, S., 2022. A Decision Support System for Cyber Physical Systems under Disruptive Events: Smart Building Application, in: *2022 IEEE International Smart Cities Conference (ISC2)*, pp. 1–7. doi:10.1109/ISC255366.2022.9922493.
- [45] Żebrowski, P., Couce-Vieira, A., Mancuso, A., 2022. A Bayesian framework for the analysis and optimal mitigation of cyber threats to cyber-physical systems. *Risk Analysis* 42, 2275–2290. doi:10.1111/risa.13900.